ELSEVIER

0958-9465(95)00006-2

Cement & Concrete Composites **17** (1995) 207–218

0958-9465/95/$9.50

A Semi-Empirical Approach to Predict Shear Strength of Ferrocement

P. Desayi & N. Nandakumar

Department of Civil Engineering, Indian Institute of Science, Bangalore 560 012, India

(Received 5 September 1994; accepted 10 February 1995)

Abstract

Based on the observation of the formation of flexure-shear crack and web-shear crack, and the occurrence of flexure-shear failure and web-shear failure, approximate analytical expressions to predict the shear force at cracking and failure have been developed based on assuming physical models. The validity of these expressions has been examined by comparing with experimental data, and best-fit semi-empirical equations have been developed. The experimental data consisted of a total of 221 rectangular specimens tested under four point loading. Of these, 155 specimens were reinforced with wire meshes uniformly distributed in the thickness or lumped equally at top and bottom and 66 specimens with wire meshes and steel bars. The proposed semi-empirical equations are then compared with the predictive equations available in the literature. Characteristic shear strength equations also corresponding to the semi-empirical equations are proposed. In respect of those specimens failing in shear, the shear strength has also been calculated using available ACI and BS code procedures for reinforced concrete and compared.

Keywords: Beams (supports), bending, cracking (fracturing), diagonal tension, ferrocement, shear strength, tests, woven wire fabric, design.

NOTATION

a Shear span
b Width of specimen
CV Coefficient of variation
f Bending stress at a section
f_b^{cr} First crack 'fibre' strength of ferrocement in bending
f_b^u 'Fibre' stress at failure of ferrocement in bending
f_{cu} Cube compressive strength of mortar
f_t^{cr} First crack strength of ferrocement in direct tension
f_{tc} Split cylinder tensile strength of mortar
f_{tu} Ultimate strength of ferrocement in direct tension
f_{ym} Yield stress of mesh wires
h Overall depth of specimen
M Bending moment at a section
p_m Volume fraction of mesh wires in longitudinal direction
p_{bt} Volume fraction of skeletal steel bars in longitudinal direction
V Shear force
v Shear stress
V_c Cracking shear force
V_{cf} Shear force at flexure-shear crack
V_{cw} Shear force at web-shear crack
v_m Maximum shear stress
V_u Ultimate shear force
V_{uc} Calculated shear force at failure
V_{ue} Experimental shear force at failure
V_{uf} Shear force at flexure-shear failure
V_{uw} Shear force at web-shear failure
Z Section modulus

θ Inclination of the crack with the longitudinal axis of the specimen, $\tan^{-1}(h/a)$

Superscript
c Characteristic strength

INTRODUCTION

Various attempts at understanding the shear strength of ferrocement have resulted in testing of

specimens of rectangular cross-section and proposals of empirical equations for shear strength.[1-4] Studies on the physical behaviour of ferrocement specimens failing in shear, on the other hand, are few, and thus the shear behaviour of ferrocement remains to be fully explained. Most of the current procedures to predict the shear strength of ferrocement specimens, being based on empirical approaches, are probably less than fully satisfactory.

Developing an improved basis for predicting the shear strength of ferrocement specimens is an important initial step towards a better understanding of the nature of shear behaviour, both at the time of crack initiation and after cracking has taken place. In this study an attempt is made to develop a more rational approach to predict the initiation of shear cracking and shear failure in rectangular ferrocement specimens subjected to four point loading.

It has been reported that there are two types of inclined cracks, namely flexure-shear and web-shear cracks, and, correspondingly, two different modes of shear failure in ferrocement specimens.[3,4] Normally ferrocement reinforcement consists of wire meshes and bars. In this study two layouts of meshes have been considered and they are: (a) distributed throughout the thickness and (b) lumped near the extreme fibres of the specimen. Steel bars were placed in the middle of the cross-section as is normally done in the small thickness of a ferrocement element. For all these cases, based on simple physical models, attempts are made to predict the shear force at the two different types of shear cracking and modes of shear failure. The constants appearing in the derived equations are then adjusted to give a best-fit with experimental data.[3,4] The resulting equations for predicting the shear strength are thus semi-empirical in nature and their development is reported in this paper. Also the corresponding characteristic strength equations are derived for use in design.

FLEXURE-SHEAR CRACKING

Ferrocement reinforced with distributed and lumped wire meshes

Figures 1(a)–1(c) show a ferrocement specimen reinforced with distributed and lumped wire meshes, subjected to four point loading and cracked in flexure. Considering the section X–X at the flexure crack e–f in the shear span, a diagonal crack f–g will form at the top of e–f when the principal tensile stress at about mid-depth exceeds the tensile strength of the ferrocement. This crack is known as 'flexure-shear crack'. From elastic analysis the maximum shear stress at mid-depth of the section is given by

$$v_m = \frac{1{\cdot}5\,V}{bh} \tag{1}$$

where v_m is maximum shear stress, V is shear force, b is width and h is overall depth of specimen. Noting that section X–X is usually close to the loading section,

$$Va = M \tag{2}$$

where a is shear span and M is bending moment at a section. From eqns (1) and (2),

$$v_m = \frac{1{\cdot}5}{bh}\left(\frac{M}{a}\right) \tag{3}$$

The bending moment at a section is also given by

$$M = fZ \tag{4}$$

where f is the bending stress and Z is section modulus. From eqns (3) and (4),

$$v_m = \frac{1{\cdot}5}{bha}(fZ) \tag{5}$$

The magnitude of f is taken as the first crack 'fibre' strength of ferrocement in bending (f_b^{cr}).[5] Though the equation for f_b^{cr} is developed for light-

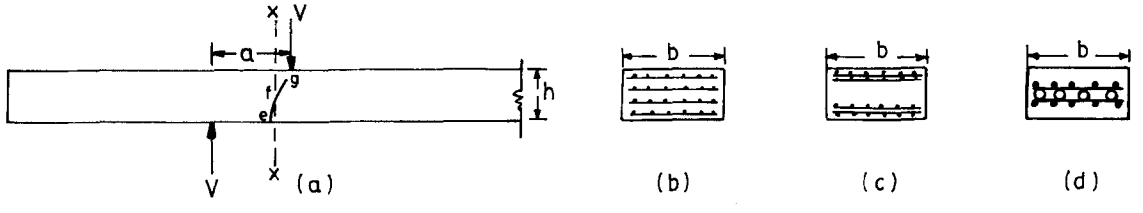

Fig. 1. Ferrocement rectangular specimen: (a) flexure-shear crack formation; (b) cross-section with distributed meshes; (c) cross-section with lumped meshes; (d) cross-section with meshes and steel bars.

weight ferrocement in Ref. 5, it was developed to be used for normalweight ferrocement also through the presence of the $\sqrt{f_{cu}}$ term. Thus, eqn (5) becomes

$$v_m = \frac{1{\cdot}5}{bha} f_b^{cr} Z \tag{6}$$

Noting, from Ref. 5,

$$f_b^{cr} = \sqrt{f_{cu}}\,(0{\cdot}712 + 64{\cdot}64\,p_m) \tag{6a}$$

and

$$Z = \frac{bh^2}{6} \tag{6b}$$

eqn (6) becomes

$$v_m = 0{\cdot}25\,\frac{\sqrt{f_{cu}}}{(a/h)}\,(0{\cdot}712 + 64{\cdot}64\,p_m) \tag{7}$$

where f_{cu} is cube compressive strength of mortar and p_m is volume fraction of mesh wires in the longitudinal direction. From eqns (1) and (7), the shear force at the formation of flexure-shear crack V_{cf} is given by

$$V = V_{cf} = 0{\cdot}17\,\frac{bh\sqrt{f_{cu}}}{(a/h)}\,(0{\cdot}712 + 64{\cdot}64\,p_m) \tag{8}$$

Ferrocement reinforced with wire meshes and steel bars

Figures 1(a) and 1(d) show a ferrocement specimen reinforced with wire meshes and steel bars, subjected to four point loading and cracked in flexure. When bars are also present they can be expected to contribute to the first crack strength of ferrocement in bending. However, there is no information on the extent of their contribution in literature. Hence, in this study, it is assumed that the bars contribute to the shear resistance in a way similar to the meshes. Hence it is assumed that f_b^{cr} of a ferrocement specimen reinforced with meshes and bars, following the study in Ref. 5, would be

$$f_b^{cr} = \sqrt{f_{cu}}\,(0{\cdot}712 + 64{\cdot}64(p_m + p_{bt})) \tag{9}$$

where p_{bt} is the volume fraction of skeletal steel bars in the longitudinal direction. Following the analysis on lines similar to that given for specimens without bars, the resulting equation for the shear force at which the flexure-shear crack occurs when the ferrocement is reinforced with wire meshes and steel bars is given by

$$V_{cf} = 0{\cdot}17\,\frac{bh\sqrt{f_{cu}}}{(a/h)}\,(0{\cdot}712 + 64{\cdot}64(p_m + p_{bt})) \tag{10}$$

FLEXURE-SHEAR FAILURE

Ferrocement reinforced with distributed and lumped wire meshes

The expression for shear force at which the flexure-shear failure occurs has been developed on lines similar to those at which flexure-shear crack occurs, with the following modifications:

(a) The maximum shear stress is taken as the nominal shear stress, i.e. the shear force V divided by the area bh (and not $1{\cdot}5\,bh$).

(b) The magnitude of f in eqn (5) is taken as the 'fibre' stress at failure of ferrocement in bending f_b^u determined in Ref. 5, viz.

$$f_b^u = \sqrt{f_{cu}}\,(0{\cdot}712 + 173{\cdot}36\,p_m) \tag{11}$$

The resulting equation for the shear force at flexure-shear failure V_{uf} for specimens reinforced with wire meshes only is of the form

$$V_{uf} = 0{\cdot}17\,\frac{bh\sqrt{f_{cu}}}{(a/h)}\,(0{\cdot}712 + 173{\cdot}36\,p_m) \tag{12}$$

Ferrocement reinforced with wire meshes and steel bars

When ferrocement specimens were reinforced with wire meshes and steel bars (Fig. 1(d)), flexure-shear failure was not noticed in the series of tests conducted and, hence, an expression for shear force at flexure-shear failure has not been developed for such specimens.

WEB-SHEAR CRACKING

Ferrocement reinforced with distributed and lumped wire meshes

Figures 2(a)–2(c) show a ferrocement specimen reinforced with distributed and lumped wire meshes subjected to four point loading and cracked in flexure in the flexure span. The web-shear crack that forms on the specimen in the shear span is assumed to be due to splitting in a fashion similar to that in the cylinder-splitting test, and the crack forms along the line joining the load

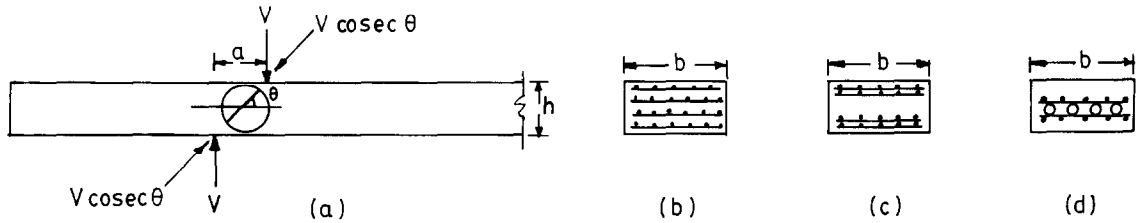

Fig. 2. Ferrocement rectangular specimen: (a) web-shear crack formation; (b) cross-section with distributed meshes; (c) cross-section with lumped meshes; (d) cross-section with meshes and steel bars.

point to the support point as shown in Fig. 2(a). If θ is the inclination of the crack with the longitudinal axis of the specimen, and the force V is resolved in the direction of the crack, the component V cosecθ in the direction of the crack causes splitting. A mortar cylinder of diameter h and height b is assumed to be split in the process. The cylinder splitting tensile stress is then given by

$$f_{tc} = \frac{2V\text{cosec}\,\theta}{\pi bh} \tag{13}$$

where f_{tc} is the split cylinder tensile strength of mortar. Noting that tensile stresses across the crack are responsible for the crack formation f_{tc} can also be taken as equal to the first crack strength of ferrocement in direct tension (f_t^{cr}) which has been determined and reported in recent studies[6] for both lightweight and normal ferrocement. From Ref. 6, f_t^{cr} is given by

$$f_t^{cr} = \sqrt{f_{cu}}\,(0{\cdot}234 + 40{\cdot}11\,p_m) \tag{14}$$

where the longitudinal wires are in the direction of loading. Since the longitudinal mesh wires are placed at an angle θ with the web-shear crack, the component of the tensile stress resisted in a direction perpendicular to the crack by them is obtained by replacing p_m in eqn (14) by $p_m \sin\theta$. Hence,

$$f_{tc} = f_t^{cr} = \sqrt{f_{cu}}\,(0{\cdot}234 + 40{\cdot}11\,p_m \sin\theta) \tag{15}$$

From eqns (13) and (15), the shear force at the formation of web-shear crack V_{cw} is given by,

$$V = V_{cw} = 1{\cdot}57\,\frac{bh\sqrt{f_{cu}}}{\sqrt{(a/h)^2+1}}\,(0{\cdot}234 + 40{\cdot}11\,p_m \sin\theta) \tag{16}$$

Ferrocement reinforced with wire meshes and steel bars

Figures 2(a) and 2(d) show a ferrocement specimen reinforced with wire meshes and steel bars subjected to four point loading and cracked in flexure in the flexure span. The web-shear crack that forms in the shear span is again assumed to be due to splitting as explained in the previous section. When bars are also present, they can be expected to contribute to the first crack strength of ferrocement in splitting but there is no information on their contribution in literature. Hence, in this study, it is assumed that the bars contribute to the shear resistance in a way similar to the meshes. Hence it is assumed that f_t^{cr} of a ferrocement specimen reinforced with meshes and bars, following the study in Ref. 6, would be

$$f_t^{cr} = \sqrt{f_{cu}}\,(0{\cdot}234 + 40{\cdot}11\,(p_m + p_{bt})\sin\theta) \tag{17}$$

Following the analysis on lines similar to those in the previous section, the resulting equation for predicting the shear force at which the web-shear crack occurs when the ferrocement is reinforced with wire meshes and steel bars is given by

$$V_{cw} = 1{\cdot}57\,\frac{bh\sqrt{f_{cu}}}{\sqrt{(a/h)^2+1}}\,(0{\cdot}234 + 40{\cdot}11(p_m + p_{bt})\sin\theta) \tag{18}$$

WEB-SHEAR FAILURE

Ferrocement reinforced with distributed and lumped wire meshes

The shear force at web-shear failure has been determined on lines similar to that of web-shear cracking. Equation (13) is again applied, with the left hand side replaced by f_{tu}, equal to the ultimate tensile strength of ferrocement in direct tension. This is equal to the tensile strength offered by mortar over the area (bh) and the wires stressed to their ultimate. The splitting tensile strength of mortar was obtained equal to 0·249 $\sqrt{f_{cu}}$ from splitting tests conducted on mortar cubes in the laboratory. The tensile force resisted in a direction perpendicular to the crack by longitudinal wire meshes is $p_m bhf_{ym} \sin\theta$, since these wires are inclined at an angle θ to the web-shear crack. Thus, f_{tu} is given by

$$f_{tu} = \frac{0{\cdot}249\sqrt{f_{cu}}bh + p_m bhf_{ym}\sin\theta}{bh} \tag{19}$$

where f_{ym} is the yield stress of mesh wires. Now, from eqns (13) and (19), the shear force at web-shear failure of ferrocement V_{uw} is given by

$$V = V_{uw} = 1{\cdot}57 \frac{bh}{[(a/h)^2 + 1]} [(0{\cdot}249\sqrt{f_{cu}}) \sqrt{(a/h)^2 + 1} + p_m f_{ym}] \quad (20)$$

Ferrocement reinforced with wire meshes and steel bars

When ferrocement specimens were reinforced with wire meshes and steel bars (Fig. 2(d)), only one specimen failed in web-shear failure mode in the series of tests conducted, and hence the resulting equation for shear force at web-shear failure has not been developed for such specimens.

EXPERIMENTAL WORK

Two series of tests on the shear strength of ferrocement have been conducted in the laboratory and a total of 221 specimens tested. These test data have been used to develop empirical equations for shear strength of ferrocement and the results have been recently reported.[3,4] The same test data have been used to finalise the equations developed so far in the present paper. The experimental work related to this is presented briefly below.

In the first series of tests, 155 specimens were tested under four point loading. The variables of the study were the mesh layout, the number of layers of wire mesh, strength of the mortar and shear span–depth ratio. The two mesh layouts used are uniformly distributed in the thickness and lumped equally at the top and bottom of the specimen. The number of layers of wire mesh is varied to get a different volume fraction of mesh wires in the longitudinal direction (p_m) and the range of p_m investigated is 0·24–1·87%. The mortar mix proportions and water–cement ratio were varied to achieve different compressive strengths (f_{cu}) and the range of f_{cu} is 20·8–45·6 MPa. The shear span–depth ratios (a/h) chosen were 0·5, 0·75, 1·0, 1·25, 1·5, 1·75, 2·0, 2·5 and 3·0. During testing, the initiation of crack in flexure span and in shear span were observed carefully and the corresponding loads recorded. The ultimate load and mode of failure were noted at failure. All test observations have been already presented.[3]

In the second series of tests the influence of skeletal steel on the shear strength of ferrocement was investigated by testing 66 specimens under four point loading. The variables of the study were the volume fraction of skeletal bars (p_b) and shear span–depth ratio (a/h). The number and diameter of bars were varied to get different p_b values and the range was 1·01–5·03%. In this study, the bars were placed at the centroidal axis of the cross-section as it occurs in normal ferrocement constructions. Two layers of wire mesh, one above and one below the bars, were placed and tied to the bars by binding wire. The a/h ratios chosen were 0·5, 0·75, 1·0, 1·25 and 1·5. All the specimens were simply supported over 600 mm length and tested under two symmetrical point loads. During testing, the initiation of cracks in flexure and shear spans was observed carefully and the corresponding load recorded. The ultimate load and mode of failure were noted at failure. The shear force at which cracks formed in shear span and/or shear failure occurred are given in Table 1. Some specimens failed in flexure and the ultimate loads of such specimens are not given, to avoid confusion.

RESULTS AND DISCUSSION

The shear force at flexure-shear cracking, web-shear cracking, flexure-shear failure and web-shear failure has been calculated for the different cases of ferrocement reinforcement using eqns (8), (10), (12), (16), (18) and (20) and compared with experimental data. It was found that eqn (8) was slightly underestimating V, eqn (10) gave almost concordant values and the rest of the equations slightly overestimated V. So, a statistical best-fit has been made between the developed expression and the experimental data for all the six cases separately and the corresponding multiplier constants determined. The resulting equations are eqns (21)–(26) and are given in Table 2. Figure 3(a) shows the shear force at flexure-shear cracking when the shear force of ferrocement reinforced with distributed and lumped wire meshes is plotted against $bh\sqrt{f_{cu}}$ $(0{\cdot}712 + 64{\cdot}64\ p_m)/(a/h)$ and the best-fit line given by eqn (21) is also superimposed with experimental results for comparison. On similar lines the plots are made for flexure-shear cracking, web-shear cracking, flexure-shear failure and web-shear failure for the different reinforcements and they are shown in Figs 3(b)–3(f). Table 2 gives the six best-fit equations and also reinforcement type, number of test data, correlation coefficient and

Table 1. Details of test results of specimens reinforced with meshes and steel bars

Specimen no.	*Bar reinforcement*†	f_{cu} *(MPa)*	*a/h*	*Shear force*		*Shear at failure (kN)*	*Mode of failure*‡
				Flexure-shear crack (kN)	*Web-shear crack (kN)*		
1	*2*	*3*	*4*	*5*	*6*	*7*	*8*
1		19·8	1·5	3·41	—	—	F
2		19·8	1·25	3·41	—	—	F
3	2–4 mm	19·8	1·0	4·89	—	—	F
4		19·8	0·75	6·82	11·37	—	F
5		19·8	0·5	—	17·05	—	F
6		19·8	1·5	4·55	—	—	F
7		19·8	1·25	4·55	—	—	F
8	4–4 mm	19·8	1·0	—	7·96	—	F
9		19·8	0·75	7·96	14·77	—	F
10		19·8	0·5	—	18·18	41·14	S
12		19·8	1·25	3·41	7·96	—	F
13	6–4 mm	19·8	1·0	—	9·09	—	F
15		19·8	0·5	—	22·73	—	F
16		19·52	1·5	2·84	—	—	F
17	2–6 mm	19·52	1·25	5·68	6·82	—	F
19		19·52	0·75	6·25	—	—	F
20		19·52	0·5	—	16·48	—	F
21		19·52	1·5	4·55	4·55	—	F
22		19·52	1·25	2·27	—	—	F
23	8–3 mm	19·52	1·0	—	7·96	—	F
24		19·52	0·75	8·52	14·77	—	F
25		19·52	0·5	—	18·18	—	F
26		19·52	1·5	2·05	—	—	F
27	2–4 mm	19·52	1·25	2·50	5·68	6·59	F-S
28		19·52	1·0	2·95	—	—	F
30		19·52	0·5	—	14·77	19·32	S
31		14·09	1·5	1·70	—	—	F
33	2–4 and 4–3 mm	14·09	1·0	2·27	—	—	F
34		14·09	0·75	—	10·23	—	F
35		14·09	0·5	10·23	—	—	F
36		14·09	1·5	2·84	6·82	—	F
37		14·09	1·25	1·70	—	—	F
38	2–4 and 1–6 mm	14·09	1·0	3·98	—	—	F
39		14·09	0·75	—	11·37	—	F
40		14·09	0·5	—	11·37	—	F
42		14·09	1·25	2·84	—	—	F
43	2–6 mm	14·09	0·5	—	13·64	—	F
44		14·09	0·5	10·23	13·64	—	F
46	2–4 mm	14·09	0·5	—	10·23	—	F
47	6–4 mm	14·09	0·5	—	17·62	—	F
48		14·09	0·5	—	13·64	—	F
49		20·94	1·25	5·11	9·09	—	F
50		20·94	1·25	5·68	9·09	—	F
51	8–3 mm	20·94	0·5	6·82	—	—	F
52		20·94	0·5	—	14·77	—	F
53	2–4 mm	20·94	1·0	2·84	—	—	F
57		20·94	1·5	2·84	—	—	F
58		20·94	1·25	2·84	—	—	F
59	8–4 mm	20·94	1·0	4·55	—	—	F
60		20·94	0·75	—	13·64	—	F
61		20·94	0·5	—	16·48	—	F
62		20·94	1·5	2·84	—	—	F
63	10–4 mm	20·94	1·25	3·98	—	—	F
64		20·94	1·0	6·25	—	—	F
66		20·94	0·5	—	14·77	—	F

†All specimens were reinforced with two layers of 6 × 22 mesh (0·6 mm diameter, spaced at 4·5 mm both ways) except in specimens 26–30 and 53–56, wherein mesh reinforcement was not provided. The mesh wires in specimens 1–5 and 16–25 had a proof stress of 425·34 MPa and in specimens 6–15, 31–52 and 57–66 had a proof stress of 407·02 MPa, respectively.
‡F, Flexural failure; F-S, flexure-shear failure; S, web-shear failure.

Table 2. Best-fit equations proposed for shear force at cracking and failure

Eqn No.	*Reinforcement*	*No. of test data*	*Best-fit equation*	*Correlation coefficient*	*Ratio of calculated–experimental shear force*	
					Mean	*CV (%)*
21	Distributed meshes and lumped meshes	41 and 17	$V_{cf}=0{\cdot}214\dfrac{bh\sqrt{f_{cu}}}{(a/h)}(0{\cdot}712+64{\cdot}64p_m)$	0·90	1·01	17·8
22	Bars and meshes at centre	35	$V_{cf}=0{\cdot}173\dfrac{bh\sqrt{f_{cu}}}{(a/h)}(0{\cdot}712+64{\cdot}64(p_m+p_{bt}))$	0·68	1·10	40·13
23	Distributed meshes and lumped meshes	4 and 1	$V_{uf}=0{\cdot}158\dfrac{bh\sqrt{f_{cu}}}{(a/h)}(0{\cdot}712+173{\cdot}36p_m)$	0·98	0·95	22·7
24	Distributed meshes and lumped meshes	39 and 13	$V_{cw}=1{\cdot}08\dfrac{bh\sqrt{f_{cu}}}{\sqrt{(a/h)^2+1}}(0{\cdot}234+40{\cdot}11p_m\sin\theta)$	0·83	1·04	23·13
25	Bars and meshes at centre	31	$V_{cw}=1{\cdot}28\dfrac{bh\sqrt{f_{cu}}}{\sqrt{(a/h)^2+1}}(0{\cdot}234+40{\cdot}11(p_m+p_{bt})\sin\theta)$	0·66	1·02	29·51
26	Distributed meshes† and lumped meshes†	7 and 1	$V_{uw}=1{\cdot}257\dfrac{bh}{[(a/h)^2+1]}((0{\cdot}249\sqrt{f_{cu}})\sqrt{(a/h)^2+1}+p_m f_{ym})$	0·78	1·03	15·6

†Details of these eight specimens failing in shear, indicated by 'S' are in Table 2 of Ref. 3. The yield strengths of the mesh wires of these specimens were 425·34, 425·34, 425·34, 443·77, 443·77, 411·07, 399·54 and 411·07 MPa in the order listed in that Table.

mean and coefficient of variation of the ratio of the calculated–experimental shear force. It is seen that the correlation coefficients and the coefficients of variation of the ratio of calculated–experimental shear for all the six cases are satisfactory except for the case when ferrocement is reinforced with wire meshes and bars. Hence, while a physical model has been used in the development of the shear strength expressions, test data were used to determine the best-fit multiplier constants and hence these equations for V are considered semi-empirical.

Comparison of the proposed method with previous models

As already reviewed, in the previous investigations empirical equations have been developed for the shear strength of ferrocement. Earlier studies have been done on ferrocement reinforced with distributed mesh, lumped mesh and meshes with bars for rectangular specimens. It was felt desirable to compare those empirical equations with the semi-empirical equations proposed in this investigation. Hence, for assumed values of $p_m=0{\cdot}0071$, $p_{bt}=0{\cdot}0101$ and $f_{cu}=25$ MPa, the variation of average shear stress, V_{cf}/bh or V_{cw}/bh, was computed and Figs 4(a)–4(c) show the comparison for the three cases separately: ferrocement reinforced with distributed mesh, ferrocement reinforced with lumped mesh and ferrocement reinforced with wire meshes and steel bars, respectively. In all these cases, it is seen that while some differences exist in the magnitudes given by the different equations all the equations show a similar trend of variation with a/h.

CRITICAL SHEAR AT CRACKING/FAILURE

When ferrocement is cracking/failing in shear, the shear force at which cracking/failure occurs is governed by the lower of the magnitudes of flexure-shear or web-shear models discussed so far. This has been examined with respect to the variation in a/h values for assumed data of test specimens.

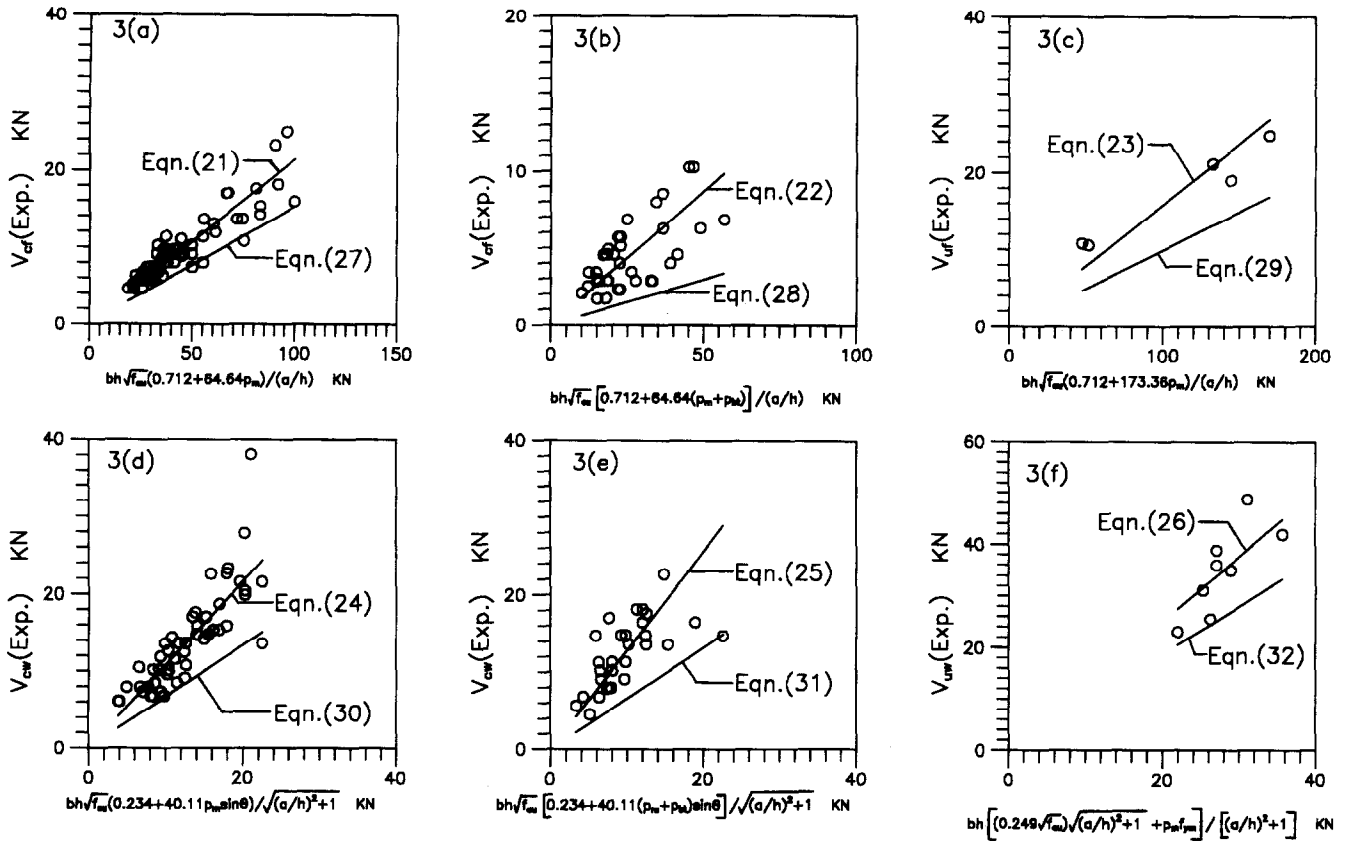

Fig. 3. Experimental points with best-fit and characteristic strength lines: (a) flexure-shear crack for specimens with distributed and lumped meshes; (b) flexure-shear crack for specimens with meshes and steel bars; (c) flexure-shear failure for specimens with distributed and lumped meshes; (d) web-shear crack for specimens with distributed and lumped meshes; (e) web-shear crack for specimens with meshes and steel bars; (f) web-shear failure for specimens with distributed and lumped meshes.

Ferrocement reinforced with distributed and lumped wire meshes

For assumed values of $p_m = 0{\cdot}0071$, $f_{cu} = 25{\cdot}0$ MPa, $b = 100$ mm and $h = 50$ mm, the shear force at flexure-shear or web-shear cracking has been calculated using eqns (21) and (24) and they are plotted with a/h in Fig. 5(a). The intersection of these two curves is approximately at $a/h = 0{\cdot}60$. Hence, for $a/h < 0{\cdot}60$, critical shear for cracking is due to a web-shear crack (eqn (24)) and for $a/h > 0{\cdot}60$ critical shear for cracking is given by flexure-shear (eqn (21)).

For assumed values of $p_m = 0{\cdot}0095$, $f_{cu} = 35{\cdot}0$ MPa, $b = 100$ mm, $h = 50$ mm and $f_{ym} = 400$ MPa, Fig. 5(b) shows the plots of eqns (23) and (26) in respect of shear failure, and the critical shear at failure is governed by eqn (23) for all a/h values.

Ferrocement reinforced with wire meshes and steel bars

For assumed values of $p_m = 0{\cdot}0048$, $p_{bt} = 0{\cdot}0101$, $f_{cu} = 25{\cdot}0$ MPa, $b = 100$ mm and $h = 25$ mm, the shear force at flexure-shear or web-shear cracking has been calculated using eqns (22) and (25) and they are plotted with a/h in Fig. 5(c). It is seen that, for all a/h values, critical cracking shear is given by the flexure-shear crack (eqn (22)).

Critical shear at failure for ferrocement having this reinforcement has not been discussed further here since no equation could be developed for shear force at failure for such a case. In general, the shear force at cracking/failure is calculated by both flexure-shear and web-shear and the lower shear force is taken as the critical shear.

CHARACTERISTIC SHEAR STRENGTH OF FERROCEMENT

Based on the best-fit equations and the mean and coefficient of variation of the computed ratio of predicted–experimental shear force (Table 2), equations for the characteristic strength (a lower strength limit, below which not more than 5% of the test results can be expected to fall) are derived to predict the shear forces at the two types of shear cracking and failure. The equations thus

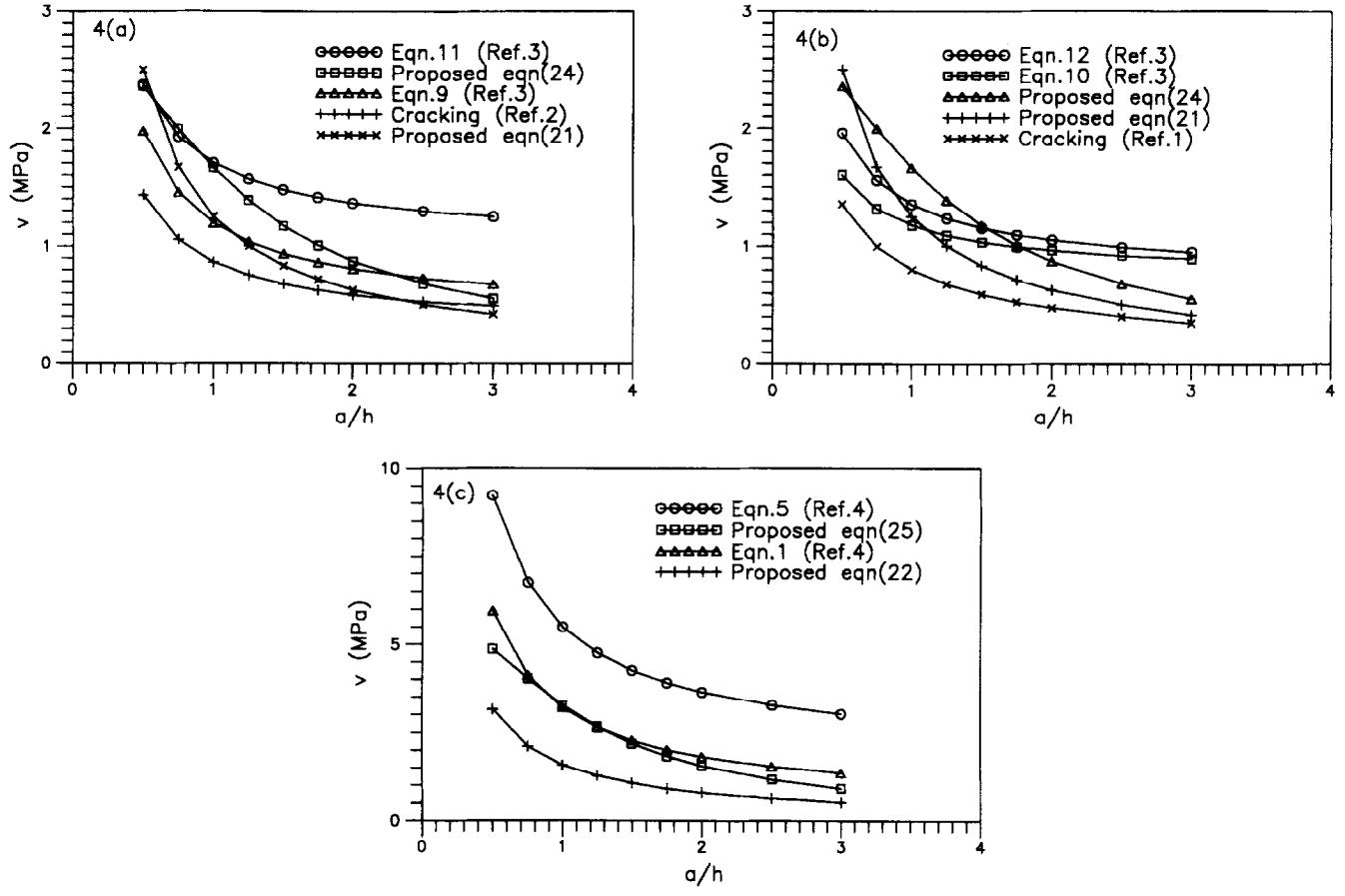

Fig. 4. Comparison of proposed equations with empirical equations in the literature: (a) specimens with distributed meshes; (b) specimens with lumped meshes; (c) specimens with meshes and steel bars.

obtained giving the characteristic shear strength are as follows:

$$V_{cf}^{c} = 0{\cdot}152 \frac{bh\sqrt{f_{cu}}}{a/h}(0{\cdot}712 + 64{\cdot}64\,p_m) \quad (27)$$

$$V_{cf}^{c} = 0{\cdot}059 \frac{bh\sqrt{f_{cu}}}{a/h}(0{\cdot}712 + 64{\cdot}64(p_m + p_{bt})) \quad (28)$$

$$V_{uf}^{c} = 0{\cdot}099 \frac{bh\sqrt{f_{cu}}}{a/h}(0{\cdot}712 + 173{\cdot}36\,p_m) \quad (29)$$

$$V_{cw}^{c} = 0{\cdot}67 \frac{bh\sqrt{f_{cu}}}{\sqrt{(a/h)^2+1}}(0{\cdot}234 + 40{\cdot}11\,p_m \sin\theta) \quad (30)$$

$$V_{cw}^{c} = 0{\cdot}66 \frac{bh\sqrt{f_{cu}}}{\sqrt{(a/h)^2+1}}(0{\cdot}234 + 40{\cdot}11(p_m + p_{bt})\sin\theta) \quad (31)$$

$$V_{uw}^{c} = 0{\cdot}935 \frac{bh}{[(a/h)^2+1]}((0{\cdot}249\sqrt{f_{cu}})\sqrt{(a/h)^2+1} + p_m f_{ym}) \quad (32)$$

The characteristic strength lines for the shear force at flexure-shear and web-shear crack/failure, viz. eqns (27)–(32), are shown in Figs 3(a)–3(f) for comparison. With suitable partial safety factors for cracking and ultimate load, the characteristic strength equations can be used to determine the design strength in the design of ferrocement against cracking and failure in shear.

SHEAR STRENGTH FROM REINFORCED CONCRETE CODES AND COMPARISON

In the guidelines for design of ferrocement reported by ACI committee 549,[7] there is no

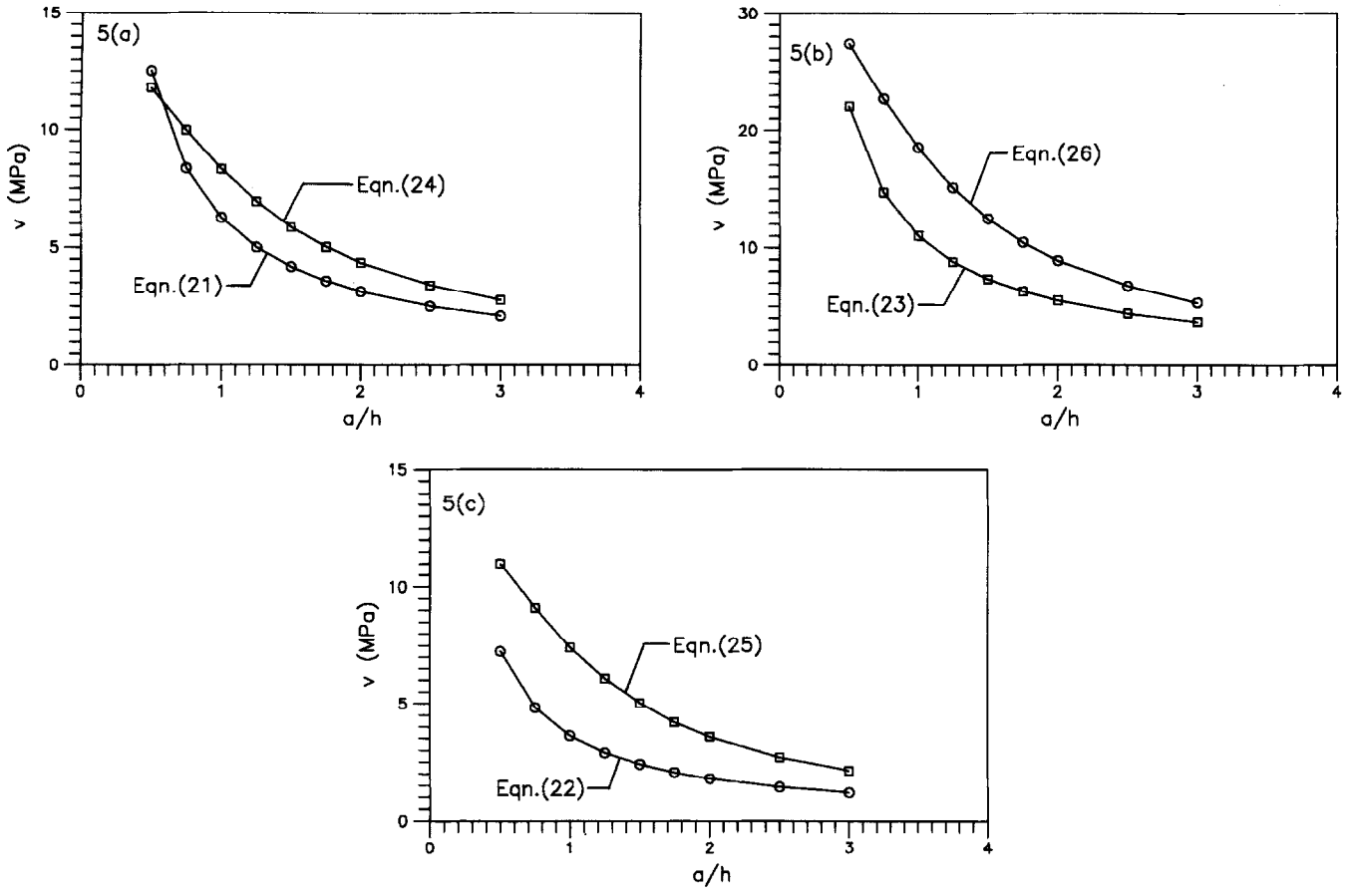

Fig. 5. Variation of critical shear with a/h: (a) at cracking for specimens with distributed and lumped meshes; (b) at failure for specimens with distributed and lumped meshes; (c) at cracking for specimens with meshes and steel bars.

suggestion for shear strength determination. Hence, it was decided to estimate the shear strength of ferrocement specimens using the guidelines given for reinforced concrete in different codes. In the present study, the experimental ultimate shear strength of ferrocement specimens is compared with the shear strength determined using the procedures given in ACI:318[8] and BS:8110[9] for the shear strength of reinforced concrete. The effective depth d is replaced by the overall depth h of the specimen. The area of longitudinal tension reinforcement A_s is taken equal to the sum of the longitudinal mesh wires in the lower half of the section and full area of steel bars. For specimens failing in shear for $a/h \leq 1{\cdot}0$, the equations given for the shear strength of brackets and corbels have been used. The shear strength so predicted has been compared with experimental shear strength and the ratio of calculated–experimental shear force is given in Table 3. The mean and coefficient of variation of the ratio for each mode of failure and for different codes are also presented in Table 3. It is seen that the codes predict the shear force at flexure-shear failure better than at web-shear failure. As expected both ACI and BS codes are conservative in predicting the shear force at failure.

Shear strength has also been computed using characteristic eqns (29) and (32) proposed in this paper and compared with test data in Table 3. It is seen that the characteristic strength equations also are conservative in estimating the shear force. The margin of safety is noted to be more for flexure-shear than for web-shear failure.

CONCLUSIONS

The following conclusions can be drawn from this investigation.

(1) Based on simple mechanistic models, the expressions to predict the shear force at flexure-shear cracking, web-shear cracking and the corresponding two failures have

Table 3. Calculated shear strength with codes and proposed characteristic equations

Source of test data	*Mode of failure*†	V_{ue} *(kN)*	*ACI:318*		*BS:8110*		*Proposed characteristic equations (eqns (29) and (32))*	
			V_{uc} *(kN)*	$\frac{V_{uc}}{V_{ue}}$	*(kN)*	$\frac{V_{uc}}{V_{ue}}$	V_{uc} *(kN)*	$\frac{V_{uc}}{V_{ue}}$
A	FS	10·57	3·17	0·3	6·35	0·60	5·09	0·48
B	FS	6·59	1·49	0·23	3·17	0·48	—	—
A	FS	18·93	23·38	1·24	18·97	1·00	14·28	0·75
A	FS	24·78	23·38	0·94	20·45	0·83	16·80	0·68
A	FS	21·14	21·42	1·01	17·92	0·85	13·11	0·62
A	FS	10·80	15·96	1·48	7·53	0·70	4·66	0·43
			Mean = 0·87 *CV* = 58·2%		Mean = 0·74 *CV* = 25·3%		Mean = 0·59 *CV* = 22·7%	
A	S	36·03	23·38	0·65	20·34	0·56	25·25	0·70
A	S	38·87	23·38	0·60	20·34	0·52	25·25	0·65
A	S	48·76	23·38	0·48	21·62	0·44	29·06	0·60
A	S	23·07	14·13	0·61	16·59	0·72	20·51	0·89
A	S	25·57	14·13	0·55	17·88	0·70	24·50	0·96
A	S	35·01	15·96	0·46	19·01	0·54	27·03	0·77
A	S	41·94	18·41	0·44	20·81	0·50	33·36	0·80
A	S	31·14	17·46	0·56	18·04	0·58	23·57	0·76
B	S	41·14	6·73	0·16	8·90	0·22	—	—
B	S	19·32	6·64	0·34	8·84	0·46	—	—
			Mean = 0·49 *CV* = 30·2%		Mean = 0·52 *CV* = 27·0%		Mean = 0·76 *CV* = 15·6%	

A, Data from Table 2 of Ref. 3.
B, Data from Table 1 of this paper.
†FS: flexure-shear failure; S: web-shear failure.

been developed. These expressions have been adjusted for a best-fit with experimental data and the corresponding semi-empirical equations proposed to predict the shear force at cracking and failure for the different cases of ferrocement reinforcement. All these equations can be used satisfactorily to predict the shear force at cracking and failure. The shear stress at cracking given by these equations and by the empirical equations existing in the literature are studied with respect to the important parameter, viz. a/h for comparison. All the equations show a similar trend of variation with a/h.

(2) The shear force has to be calculated by both flexure-shear and web-shear models and the lower value is to be taken as the critical resisting shear force. This critical shear force is normally found to be governed by flexure-shear.

(3) From the semi-empirical equations, characteristic strength equations have been proposed to predict the shear strength of ferrocement at flexure-shear cracking, web-shear cracking, flexure-shear failure and web-shear failure. Suitable partial safety factors for cracking and ultimate can be used with these characteristic strength equations for designing ferrocement against shear.

(4) The expressions given in ACI and BS code for shear calculations are for reinforced concrete. In this study, the same expressions have been used for calculating the shear strength of ferrocement specimens in the absence of any codal methods of computing shear strength of ferrocement. It is noticed that, the procedures given in these two codes are conservative and underestimate the shear force at flexure-shear and web-shear failure. The underestimation for web-shear failure is more than that for flexure-shear failure.

REFERENCES

1. Mansur, M. A. & Ong, K. C. G., Shear strength of ferrocement beams. *ACI Struct. J.*, **84** (1) (1987) 10–17.
2. Venkatakrishna, H. V. & Gouda, P. B., Some studies on the behaviour of ferrocement in shear. *Proc. 3rd Int. Symp. on Ferrocement*, New Delhi, Dec. 1988, pp. 99–105.
3. Desayi, P., Nanda Kumar, N. & El-kholy, S. A., Strength and behaviour of ferrocement in shear. *Cement and Concrete Composites*, **14** (1) (1992) 33–45.
4. Desayi, P. & Nandakumar, N., Influence of skeletal steel on the shear strength of ferrocement. *Int. Symp. on Innovative World of Concrete*, Proceedings Vol. II, Ch. 3, Oxford & IBH Pub. Co., New Delhi, pp. 151–9.
5. Desayi, P. & El-kholy, S. A., First crack strength and modulus of rupture of lightweight fibre reinforced ferrocement in flexure. *J. Ferrocement*, **22** (2) (1992) 151–61.
6. Desayi, P. & El-kholy, S. A., Lightweight fibre-reinforced ferrocement in tension. *Cement and Concrete Composites*, **13** (1991) 37–48.
7. ACI Committee 549 Report. Guide for the design, construction and repair of ferrocement. (ACI Committee 549). *ACI Struc. J.*, **85** (3) (1988) 325–51.
8. ACI Committee 318, *Building Code Requirements for Reinforced Concrete* (ACI 318-89). American Concrete Institute, Detroit, 1989, pp. 351.
9. *Structural Use of Concrete* (BS 8110: Part 1). British Standards Institution, London, 1985.
10. ACI-ASCE Committee 426 Report. The shear strength of reinforced concrete members. *J. Struct. Division, ASCE*, **99** (ST6) (1973) 1091–187.